Natural Resources Canada | Ressources naturelles Canada

GEOLOGICAL SURVEY OF CANADA
OPEN FILE 8106

A Comparison of Seismicity to the Crustal Deformation Predicted by a Glacial Isostatic Adjustment Model in northern Canada and western Greenland

T.S. James and T.D. Schamehorn

2016

GEOLOGICAL SURVEY OF CANADA
OPEN FILE 8106

A Comparison of Seismicity to the Crustal Deformation Predicted by a Glacial Isostatic Adjustment Model in northern Canada and western Greenland

T.S. James and T.D. Schamehorn

Geological Survey of Canada, Pacific Division, Sidney, BC, Canada

2016

doi:10.4095/299098

This publication is available for free download through GEOSCAN (http://geoscan.nrcan.gc.ca/).

Recommended citation
James, T.S. and T.D. Schamehorn, 2016. A comparison of seismicity to the crustal deformation predicted by a glacial isostatic adjustment model in northern Canada and western Greenland; Geological Survey of Canada, Open File 8106, 1 .zip file. doi:10.4095/299098.

Publications in this series have not been edited; they are released as submitted by the author.

ABSTRACT

The horizontal crustal strain-rates induced by glacial isostatic adjustment (GIA) in northern Canada and western Greenland region are compared to the spatial pattern of seismicity to determine whether earthquakes occur where GIA-predicted crustal strain-rates are high. For the comparison, an updated seismicity catalogue was created from the 2010 version of the NRCan Seismic Hazard Earthquake Epicentre File (SHEEF2010) catalogue and the Greenland Ice Sheet Monitoring Network (GLISN) catalogue of the Geological Survey of Denmark and Greenland (GEUS). Crustal motion rates were computed using the Innu/Laur16 ice-sheet history and the VM5a viscosity profile. This GIA model optimizes the fit to relative sea-level and vertical crustal motion measurements around Hudson Bay and the Canadian Arctic Archipelago (CAA). A region in Baffin Bay where predicted GIA strain-rates are high also features historically high seismicity, including the 1933 M 7.4 and the 1934 and 1945 M 6.5 earthquakes. Elsewhere, agreement is not strong, with zones of seismicity occurring where predicted horizontal crustal strain-rates are small and large crustal strain-rates occurring where earthquake occurrence is muted. Further investigations could include calculation of crustal stress-rates so that failure criteria may be assessed for Baffin Bay events.

TABLE OF CONTENTS

FIGURES

TABLES

INTRODUCTION

Northern Canada, including the region of Baffin Island and Baffin Bay, has zones of enhanced seismicity, while other regions are seismically quiescent (e.g., Basham et al., 1977). Earthquakes in intraplate regions originate due to a variety of causes, including tectonic stresses transmitted from plate boundaries and from the base of the lithosphere and thermal stresses generated by lithospheric cooling. Spatial variations in lithospheric strength are also recognized as an extremely important factor in explaining the observed clustering of intraplate seismicity.

The solid Earth's response to ice mass change, which includes the ongoing response to past ice changes, as well as the response to present-day changes, is known as glacial isostatic adjustment (GIA). In North America and Greenland, Fennoscandia, Antarctica, and elsewhere, lithospheric loading and flexure induced by fluctuating ice sheets and glaciers are thought to potentially play an important role in the generation of intraplate earthquakes (e.g., Basham et al., 1977; Grollimund and Zoback, 2001; Chung, 2002; Ivins et al., 2003). The precise relationships between observed seismicity and GIA-induced stresses, the background stress field, lithospheric structure, and other seismogenic factors are not, however, well understood.

In this report the relationship between observed seismicity and the crustal strain-rates generated by a recently-published GIA model is explored in a preliminary manner for a large region centred on Baffin Island and encompassing much of the Canadian Arctic Archipelago, Hudson Bay, and western Greenland. First, a combined earthquake catalogue is produced from the Seismic Hazard Earthquake Epicentre File (SHEEF2010; Halchuk et al., 2015) catalogue of Natural Resources Canada and the Greenland Ice Sheet Monitoring Network (GLISN; GEUS, 2016) catalogue of the Geological Survey of Denmark and Greenland (GEUS). Second, crustal motions and derived strain-rates generated are described for a recently-published GIA model which is termed Innu/Laur16 in this report (Simon et al., 2015; 2016). Third, the observed seismicity and crustal strain-rates are qualitatively compared to determine regions where there is apparent agreement or lack of correspondence. Finally, suggestions for future work are provided.

Seismicity Catalogues

The study area is centered on the Baffin Island region and includes much of the Canadian Arctic Archipelago, Hudson Bay, and the western and southern parts of Greenland. It encompasses the region from 40°W to 100°W and 55°N to 85°N. To obtain a more complete record of seismicity in the study region, an NRCan seismicity catalogue was combined with a Greenland seismicity catalogue. The SHEEF2010 catalogue is used for seismic hazard analysis in Canada and includes events dating from 1809 to 2010 in the study region. In contrast, the GLISN catalogue contains events recorded by a regional network in Greenland between 1969 to the present (catalogue downloaded March 7, 2016) and contains events as small as M0.2. Details of the input catalogues are given in Appendix A.

Combining Earthquake Catalogues

In combining the catalogues, events later than Dec. 31, 2010 and events with a catalogue magnitude less than 2.5 in the GLISN catalogue were removed to ensure consistency with the

SHEEF2010 catalogue. Many duplicate entries were identical (time stamp, location, and magnitude) and these were readily removed. Other events were extremely similar, with differences at the level of 1 or 2 seconds for the event time, a few tens of kilometers in distance, or 1 or 2 tenths of a magnitude unit) and these were also removed through a manual process. In all cases, the SHEEF2010 event was retained and the GLISN event was removed. The final combined duplicate-free catalogue contains 3182 events from the SHEEF2010 file and 40 events from GLISN for a total of 3222 events (Figure 1).

The combined catalogue features zones of seismicity (Figure 1) described by Basham et al. (1977) for northern Canada, while Olivieri and Spada (2015) provide a recent review for Greenland. The largest earthquake, a M7.4 1933 complex strike-slip event (Bent, 2002), occurred in Baffin Bay. The two next largest events (M6.5) occurred close to the M7.4 event in 1934 and 1945 and may be aftershocks (Qamar, 1974). Elsewhere, seismicity levels are much lower, although a total of 7 earthquakes with magnitude larger than or equal to M6.0 are present in the combined catalogue (Figure 1 (inset)).

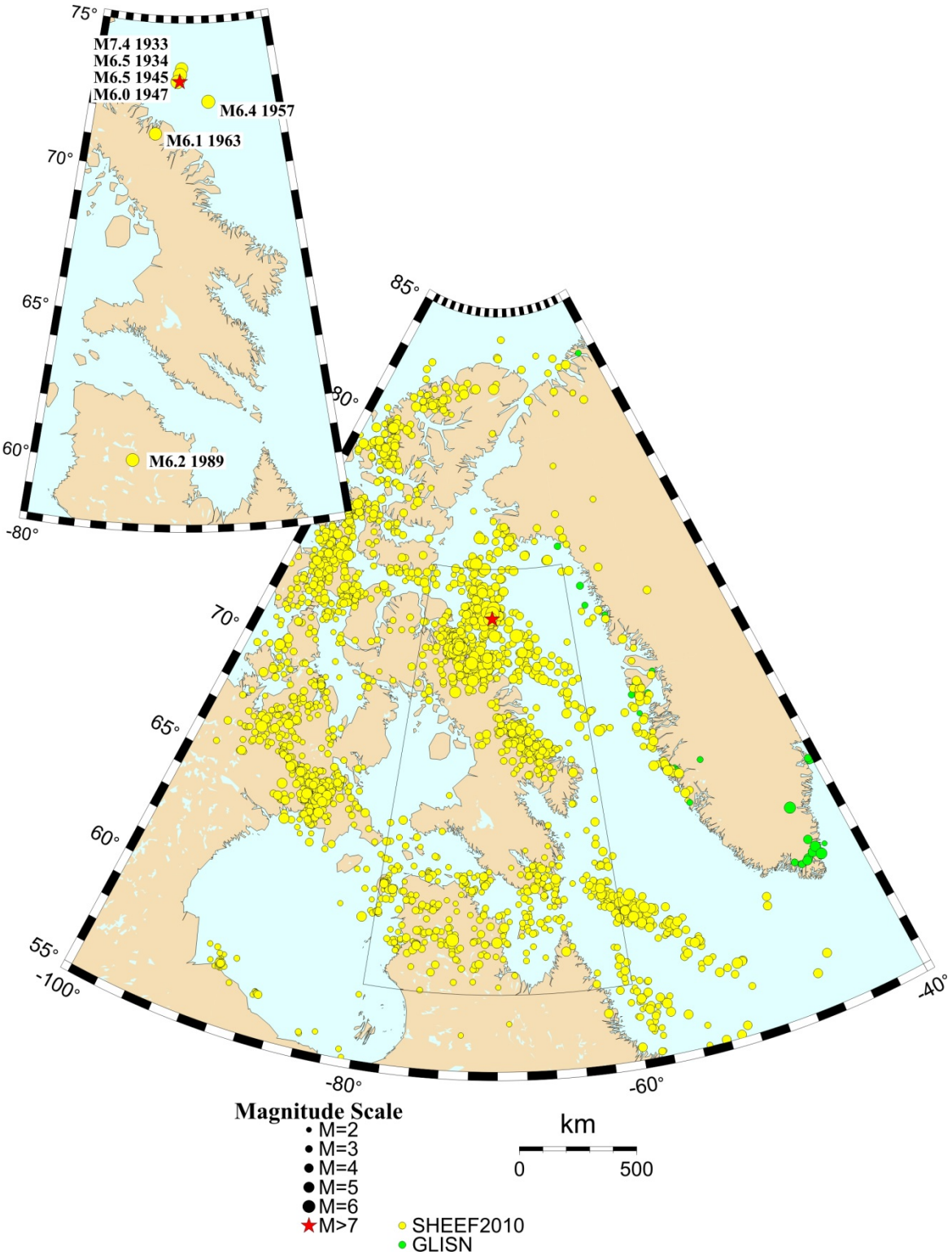

Figure 1. Plot of the final combined catalogue after removing duplicate earthquakes. The red star is the 1933 M7.4 earthquake. (inset) Locations of earthquakes in the catalogue that have magnitude 6.0 or larger.

The magnitudes of earthquakes from the GLISN catalogue were converted to moment magnitudes using the same criteria that were used for eastern Canada earthquakes in the SHEEF2010 catalogue (Allen et al., 2016):

Pre-1995:

$M_W = m_N - 0.4$

$M_W = M_L - 0.4$

All other earthquakes were treated as M_W.

Post-1995 to the end of 2010:

$M_W = m_N - 0.5$ (where $M_L = m_N$ and all other magnitudes treated as M_W)

Because of magnitude conversions, events in the combined catalogue are as small as M_W 2.0.

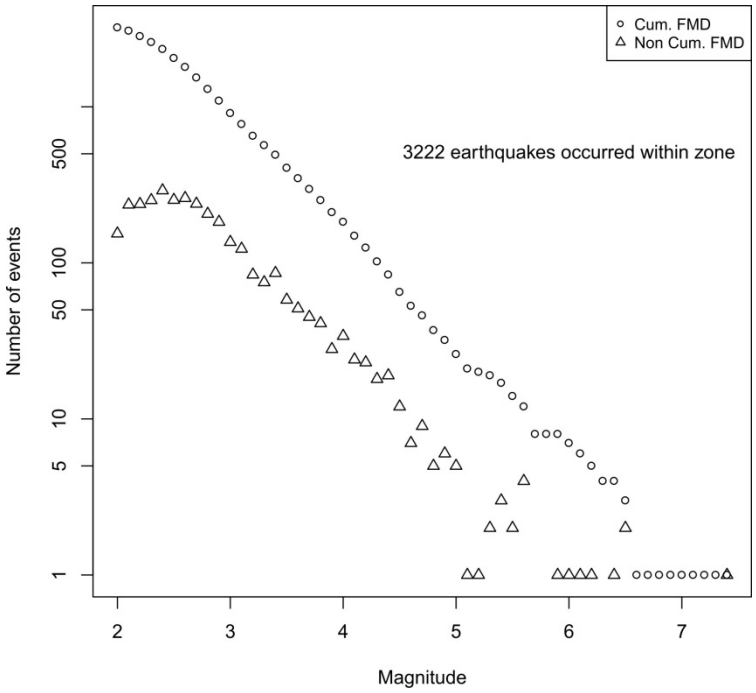

Figure 2. Frequency Magnitude Distribution (FMD) of the 3222 earthquakes present in the combined SHEEF2010 and GLISN catalogues. Triangles give the histogram of earthquake frequency (non-cumulative FMD) and circles indicate the cumulative FMD.

A histogram and cumulative frequency-magnitude distribution plot (Figure 2) of the combined catalogue shows some non-smooth behavior that is likely to be indicative of catalogue incompleteness. Seismic networks in northern Canada and Greenland were progressively densified through the 20th century.

Catalogue completeness

Catalogue completeness dates for BFB (Baffin Bay) (Table 1; Allen et al., 2016) were utilized to develop a complete catalogue for the study region, assuming it applies to the entire region. The complete catalogue was derived from the combined catalogue by removing all earthquakes smaller

than a specified magnitude that occurred earlier than the specified year of completeness (Table 1). The complete catalogue contains events of magnitude 3.3 and larger.

Table 1. Criteria for earthquakes passing completeness

Magnitudes greater than	Are complete from the year, onwards
7.35	1850
6.25	1917
5.95	1930
4.95	1951
3.25	1965

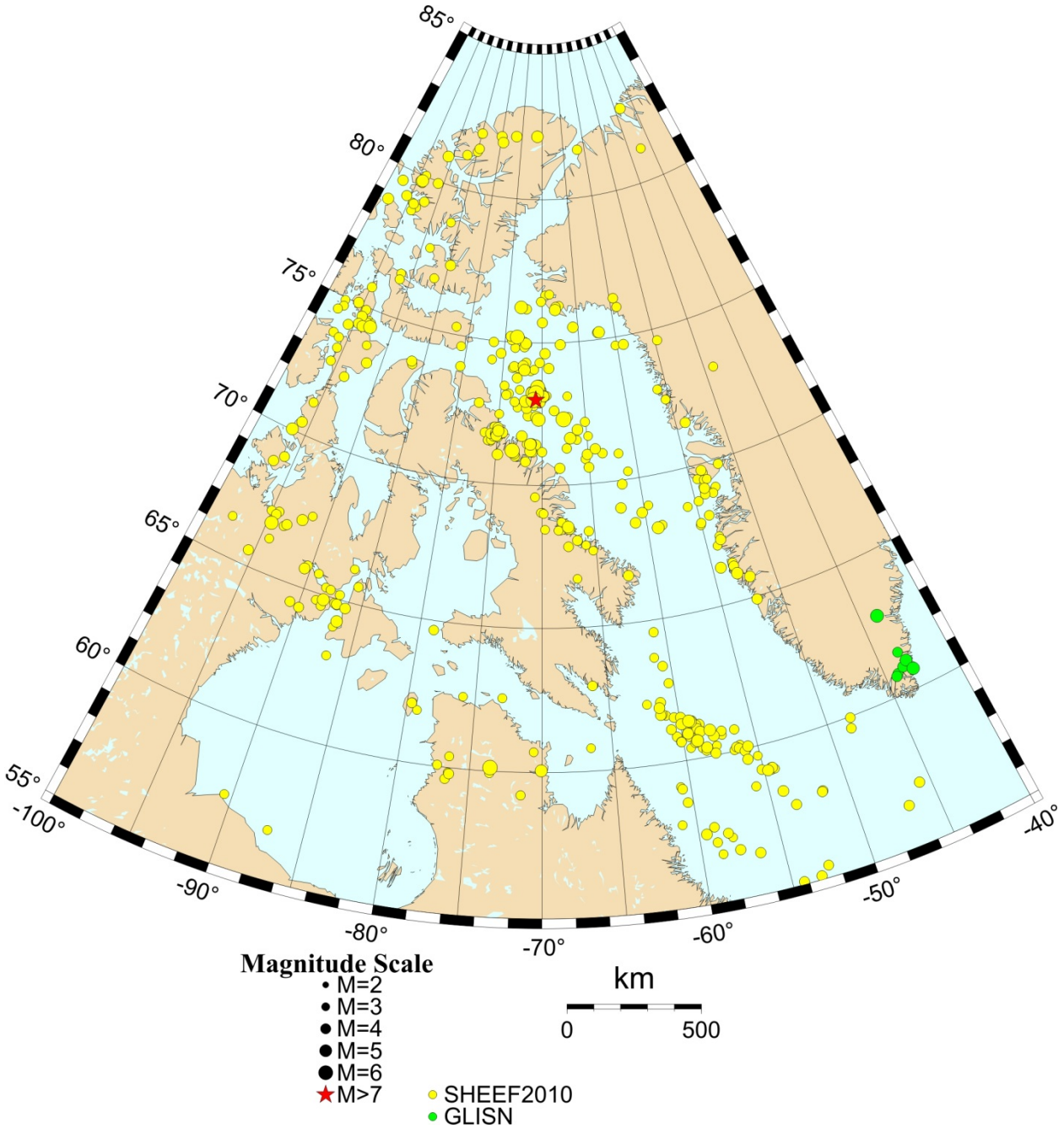

Figure 3. Plot of the earthquake catalogue after earthquakes not passing completeness have been removed.

Of the 3222 earthquakes in the combined catalogue, 497 passed completeness and are present in the complete catalogue (Figure 3). It was noted that the complete catalogue had more earthquakes of magnitude 3.4 (3.35 to 3.45) than magnitude 3.3. Consequently, in subsequent analyses, the minimum magnitude was chosen to be 3.4 and 428 events are present in this revised complete catalogue. Seismicity rates were then calculated using the earthquakes that passed completeness. For a time range of 160 years, the number of earthquakes of each magnitude was then estimated and the

frequency-magnitude plot is shown in Figure 4. For the 160-year time frame, the total estimated number of earthquakes is 1500.

The b-value was calculated for the study region using maximum-likelihood estimation (Aki, 1965).

$$b = \frac{\log_{10}(e)}{\left[\langle M \rangle - \left(M_c - {}^{\Delta M_{bin}}/_{2}\right)\right]}$$

Here $\langle M \rangle$ represents the mean magnitude of the sample and ΔM_{bin} is the binning width of the catalogue. The b-value is the negative of the slope of the best-fitting line to the cumulative distribution. For the entire study region, the b-value is 0.85 ± 0.02 (Figure 4). When the largest earthquake (M7.4) is removed, the fit changes and the b-value is 0.92 ± 0.02.

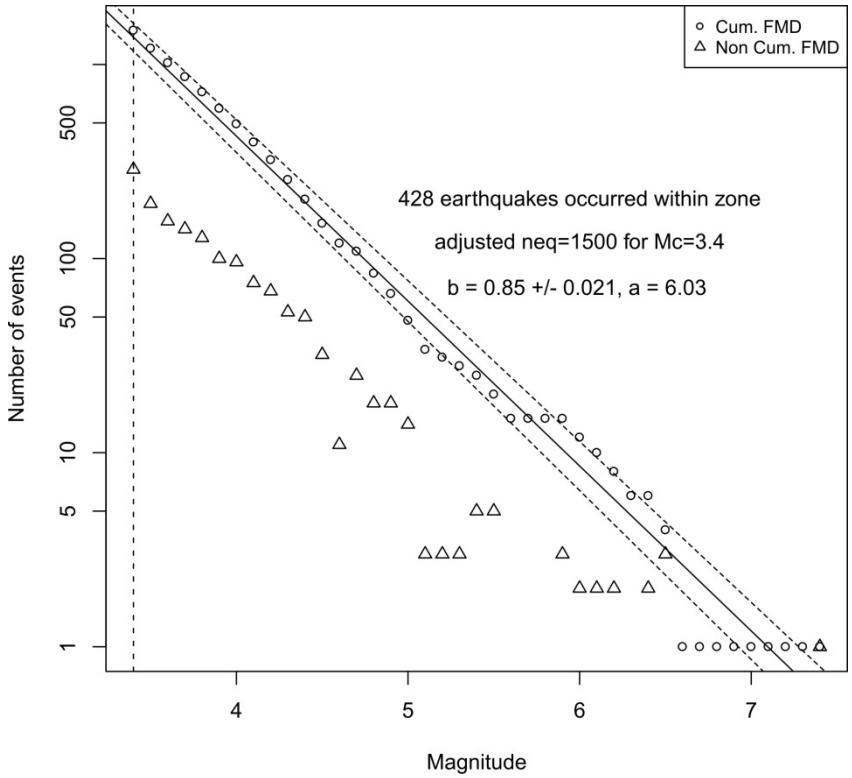

Figure 4. Frequency magnitude distribution for the M 3.4 complete catalogue normalized to 160 years. The upper and lower lines indicate one standard deviation of the calculated b-value.

Seismicity by Region

The study area was subdivided into 9 equal areas of 8.36 x 10^5 km^2 labelled A to I (Figure 5). b-values were computed for each sub-region. Two of the regions (C and G) had a small number of earthquakes passing completeness and a regression was not carried out. For the other sub-regions, b-values range from 0.68 to 1.08 (Table 2). This wide range of b-values may be more indicative of the sparseness of seismicity in the subregions than of differing processes and structural control on seismicity.

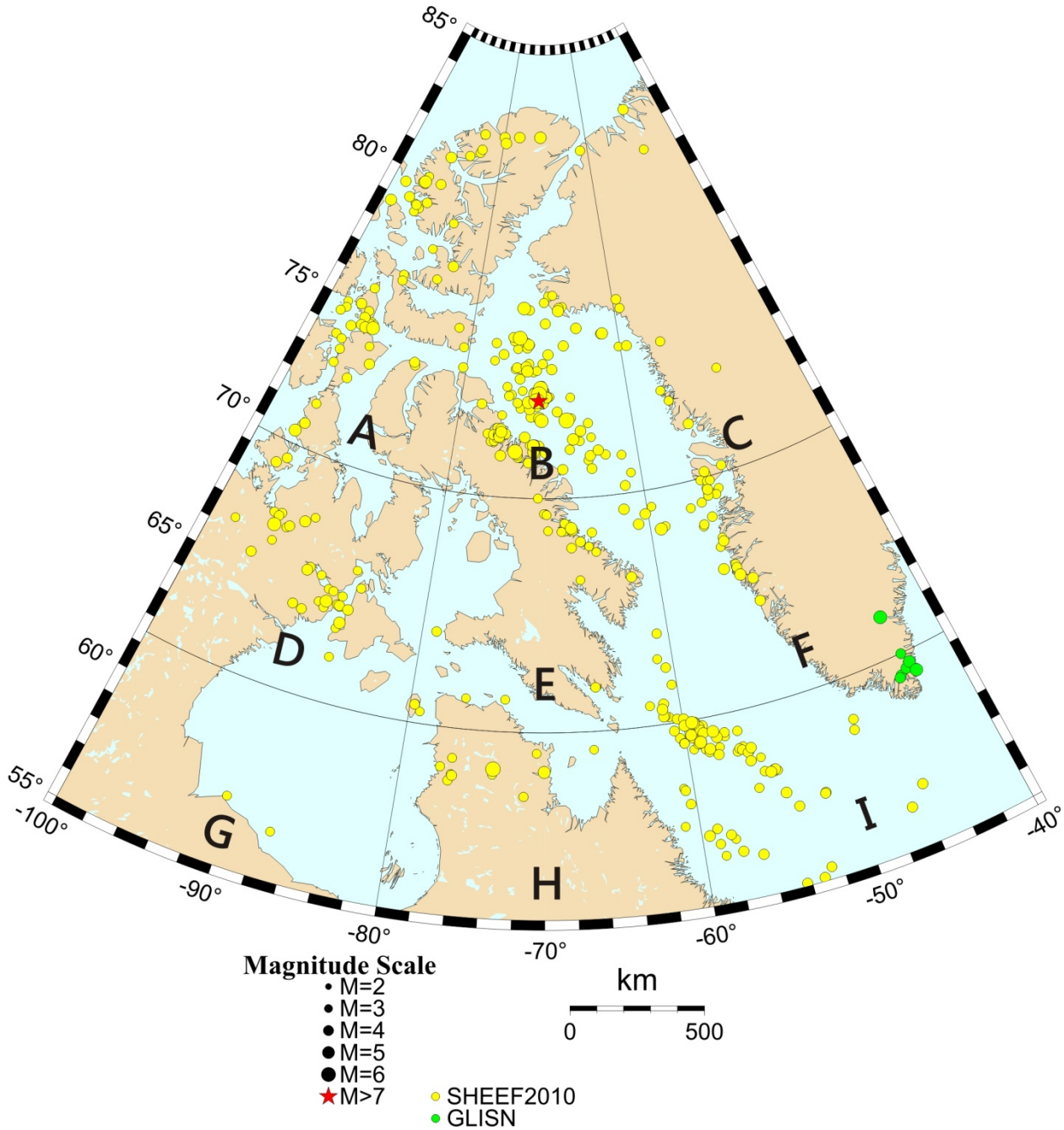

Figure 5. Equal-area sub-regions A to I are indicated with combined seismicity catalogue.

Table 2. Summary Statistics for Sub-regions

Region	a-value	b-value with standard deviation	Number of Earthquakes in Zone	Number of Earthquakes passing completeness	Number of Earthquakes for 160 years
A	5.509	0.96 ± 0.064	665	52	191
B	5.585	0.81 ± 0.04	925	157	546
C	n/a	n/a	46	13	48
D	5.042	0.86 ± 0.07	575	39	141
E	5.830	1.08 ± 0.09	470	40	144
F	5.034	0.87 ± 0.09	78	29	105
G	n/a	n/a	39	3	7
H	5.492	0.98 ± 0.13	241	23	80
I	4.588	0.68 ± 0.03	183	72	250

GIA MODEL PREDICTIONS

GIA models are comprised of a model of the ice sheet history and a model of Earth structure and rheology. Surface loading of the Earth model by the ice sheet history model is simulated and predictions of the Earth's response, including surface deformation and motion, gravitational changes, and relative sea-level change are made (e.g., Wu and Peltier, 1982; James and Ivins, 1998; Peltier, 2004; Peltier et al., 2015).

Recently, new GIA models were presented that provide an improved fit to vertical crustal motion measured by GPS and to relative sea-level observations for northern Canada (Simon et al., 2015; 2016). The new models were tuned for the Canadian Arctic Archipelago and a region surrounding Hudson Bay. They comprise the Innuitian Ice Sheet on the Queen Elizabeth Islands (Simon et al., 2015) and a large portion of the Laurentide Ice Sheet (Simon et al., 2016). For the Innuitian Ice Sheet, a new loading history model was developed from available geological and geomorphological constraints on ice sheet history. For the Laurentide ice sheet, the starting model was ICE-5G and ice thicknesses were iteratively adjusted to improve the fit with observations. The new models provide an improved fit to both vertical crustal motion measurements and relative sea-level observations over the study region relative to the ICE-5G (Peltier, 2004) and ICE-6G (Peltier et al., 2015) models (Simon et al., 2015; 2016). In this report, the two new models are combined and the combined model is termed Innu/Laur16.

Crustal motion predictions were generated for Innu/Laur16 employing the VM5a earth model. This Earth model provides an improved fit to horizontal crustal motion in North America (Peltier and Drummond, 2008) and has been employed to make predictions for ICE-5G (Argus and Peltier, 2010) and to develop ICE-6G (Peltier et al., 2015) and Innu/Laur16 (Simon et al., 2015; 2016). The viscosity profile of VM5a features viscosities of 3.2×10^{21} Pa s (lower part of the lower mantle),

1.6×10^{21} Pa s (upper part of the lower mantle), 5×10^{20} Pa s (upper mantle), and 10^{22} Pa s in a 40-km thick high-viscosity layer underlying a 60 km thick elastic lithosphere.

For computing the horizontal strain rates, a 1° × 1° degree grid was defined over the study region. For each grid point, two additional points were defined that are 0.1° to the north and to the east. Each point is referred to as a triplet, with the original point as the reference location. Crustal motion rates for each triplet were computed using the aforementioned model and viscosity profile. The results for a triplet are shown in Table 3.

Table 3: Example output from GIA earth model

Latitude (° North)	**Longitude (° East)**	**Uplift Rate (mm/yr)**	**South Velocity (mm/yr)**	**East Velocity (mm/yr)**
55.0˚	260.0˚	7.18295008	0.16851166	-0.02411362
55.1˚	260.0˚	7.25148184	0.15973753	-0.02654893
55.0˚	260.1˚	7.20850405	0.16976190	-0.02390268

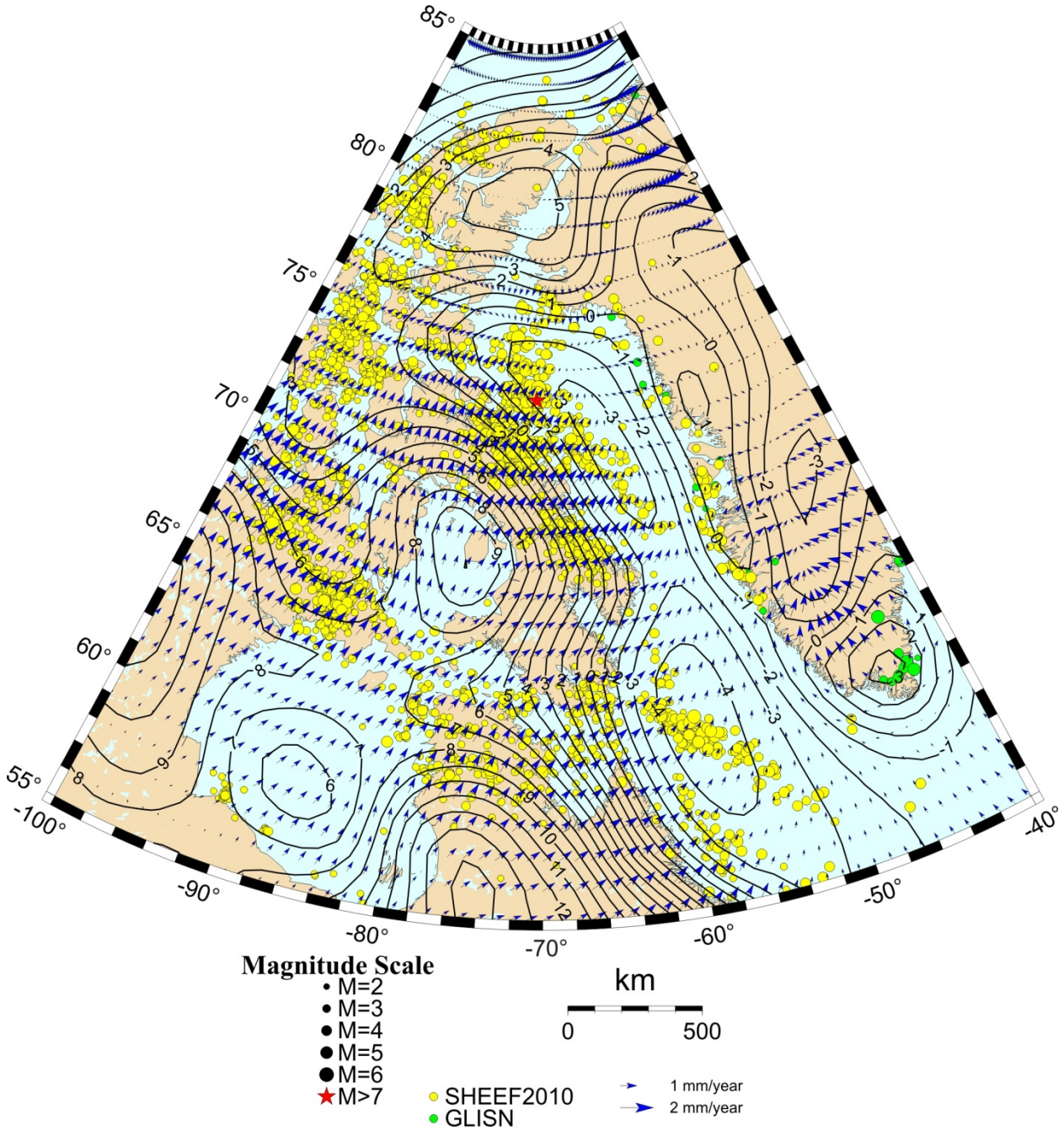

Figure 6. Predicted crustal motion for the Innu/Laur16 GIA model and VM5a Earth model. The vertical crustal motion contour interval is one millimetre per year. Horizontal motions are shown in blue arrows; scale is at bottom of figure. Also shown are the earthquakes of the combined seismicity catalogue.

The horizontal components of the strain-rate tensor in a spherical coordinate system are given by:

$$\varepsilon_{\theta\theta} = \frac{1}{r}\left(\frac{\partial u_\theta}{\partial \theta} + u_r\right)$$

$$\varepsilon_{\phi\phi} = \frac{1}{r\sin\theta}\left(\frac{\partial u_\phi}{\partial \phi} + u_r \sin\theta + u_\theta \cos\theta\right)$$

$$\varepsilon_{\theta\phi} = \frac{1}{2r}\left(\frac{1}{\sin\theta}\frac{\partial u_\theta}{\partial \phi} + \frac{\partial u_\phi}{\partial \theta} - u_\phi \cot\theta\right)$$

, where θ is co-latitude, ϕ is longitude, and r is radius, u_r, u_θ, and u_ϕ are the components of the crustal velocity vector in spherical coordinates and the surface horizontal strain rates are $\varepsilon_{\theta\theta}$, $\varepsilon_{\phi\phi}$, $\varepsilon_{\theta\phi}$. These strain-rate components correspond to strain (positive is extensional) in a north-south and east-west directions and to a rotational strain, all in the horizontal plane. Horizontal strain-rates computed on a sphere include a contribution from vertical crustal motion. Uplift contributes to horizontal extension, while subsidence contributes to horizontal compression (e.g., Malvern, 1969). Principal strain-rates and the angle of rotation were then determined for plotting purposes. The resulting strain-rates are given in figure 7.

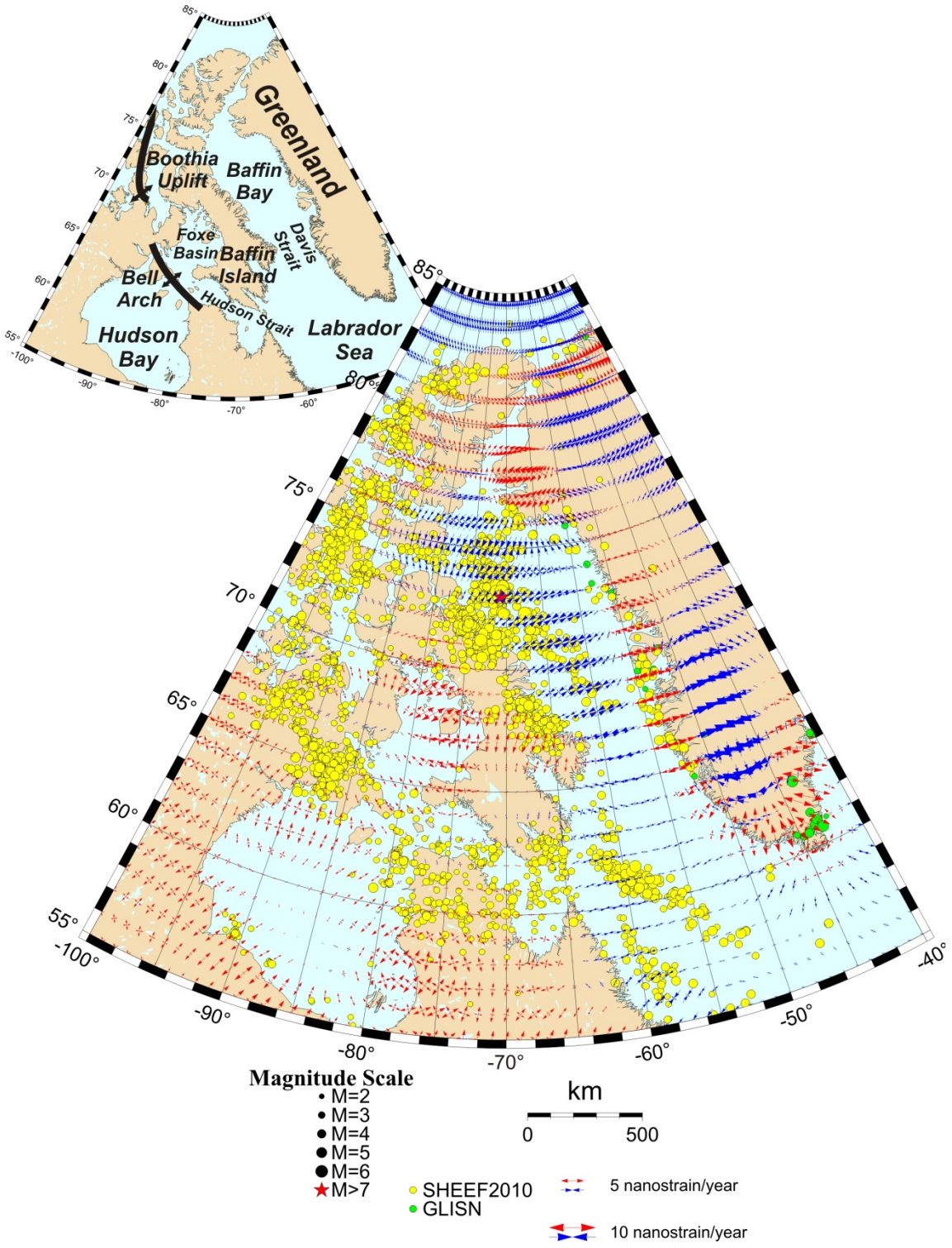

Figure 7. Predicted crustal strain-rates (crosses, red is extension and blue is compression) for the Innu/Laur16 GIA model and VM5a Earth model, superposed on the combined seismicity catalogue. Also shown is the location of the 1933 M7.4 earthquake (star). (inset) Location map giving place names and geologic features mentioned in the text.

COMPARISON OF GIA PREDICTIONS TO SEISMICITY

The predicted strain-rates range from ongoing compression of nearly -12 nanostrain/year (-12 $\times 10^{-9}$ a^{-1}) to extension of nearly +7 nanostrain/year (7×10^{-9} a^{-1}) (Figure 7). The areas of largest ongoing compression include a part of southern Greenland and most of Baffin Bay extending south into Davis Strait. Both of these regions are experiencing subsidence, and this contributes to the predicted horizontal compression. As well, northeast-directed horizontal velocities decrease from Baffin Island to Baffin Bay (Figure 6), and this contributes to ongoing horizontal compression with the largest compression oriented northeast-southwest in Baffin Bay.

Much of the study area is undergoing present-day horizontal extension, largely a consequence of widespread ongoing postglacial crustal uplift. Large ongoing extension is predicted in Foxe Basin, much of the southern portion of the study region surrounding Hudson Bay, and two portions of the western Greenland coastline. Foxe Basin and the region around southern Hudson Bay are rising rapidly and this contributes to the predicted horizontal extension (Figure 6). On the west coast of Greenland, horizontal velocities are diverging where the crustal strain-rates are extensional.

The region of largest horizontal compression in southern Greenland is seismically quiescent, in contrast to the next largest region of predicted compression in Baffin Bay, where five of the seven largest earthquakes ($M \geq 6$) in the combined catalogue occurred (Figure 1 inset). Part of northern Greenland is also undergoing crustal shortening and this region, like the region in southern Greenland, is also seismically quiescent. The seismically quiescent regions in Greenland undergoing horizontal compression may reflect suppression of seismicity due to the weight of the overlying Greenland Ice Sheet (Johnston, 1987). In Greenland, Olivieri and Spada (2015) note that most earthquakes occur on the margins of the ice sheet and attribute Greenland earthquakes to a combination of regional glacial isostatic adjustment and present-day ice sheet thinning. In Baffin Bay, the predicted ongoing postglacial horizontal compression may contribute to the observed high level of seismicity. In contrast to the possible correspondence of seismicity with high horizontal compression in Baffin Bay, the zones of large predicted crustal extension in Foxe Basin and the region around southern Hudson Bay do not correspond to regions of marked seismicity.

Elsewhere, zones of seismicity exist that do not correspond to large postglacial crustal strain rates predicted by the Innu/Laur16 model. The zone of seismicity in eastern Baffin Island corresponds to low strain rates that are transitioning from extension to the southwest in Foxe Basin to compression in Baffin Bay. An arcuate zone of seismicity that runs south from the central CAA along the Boothia Uplift (Basham et al., 1977) and curves southeast across northern Hudson Bay to Ungava in northern Quebec along the Bell Arch (Basham et al., 1977) generally corresponds to small crustal strain-rates (Figure 7 and inset). Similarly, in the Labrador Sea, a northwest-southeast oriented zone of seismicity, possibly related to an extinct spreading centre, does not correspond to large predicted crustal strain rates.

DISCUSSION AND FURTHER RESEARCH

In general, the correspondence between earthquake occurrence and large predicted GIA strain-rates is not strong, although most of the largest earthquakes in the study region have occurred in Baffin Bay where predicted horizontal GIA strain rates are large and compressional. Elsewhere, however, in

a large region that includes western Greenland and much of northeastern Canada, many zones of earthquake occurrence correspond to regions where strain rates are small. As well, several regions where predicted strain-rates are large do not correspond to zones of enhanced seismicity. This includes large compressional strain-rates underlying portions of the Greenland Ice Sheet and large extensional strain-rates in the region of southern Hudson Bay and the Foxe Basin.

The correspondence between the substantial seismicity in Baffin Bay and the large predicted crustal strain-rates warrants further investigation. In particular, predictions of the present-day change in crustal stress due to GIA, in the context of inferred P-axes from focal mechanism solutions (e.g., Bent, 2002), would enable an investigation of stress changes in terms of the Coulomb or Mogi-von Mises fracture criteria (e.g., Wu and Hasegawa, 1996; Ivins et al., 2003) to quantitatively determine the degree to which postglacial deformation is promoting seismicity in this seismically active region. More broadly, comparison of the crustal strain rates inferred from seismicity to the crustal strain and stress rates predicted by tuned GIA models could be carried out across the study region and assessed in terms of the current understanding of the crustal stress field. Estimates of the 'efficiency' of GIA-induced crustal strain could then be generated.

SUMMARY

The investigations carried out to date identify a region of large predicted GIA-induced ongoing compression in Baffin Bay that corresponds to the region of greatest seismicity in the study region. This may indicates a role for glacial isostatic adjustment in the generation of these earthquakes, as suggested in numerous previous studies (e.g., Qamar, 1974; Stein et al., 1979; Wetmiller and Forsyth, 1982). Elsewhere, however, the correspondence between GIA crustal strain and seismicity is not strong. Suggestions for further research are provided, with the key activity being calculation of crustal stress-rates so that failure criteria may be assessed for Baffin Bay events.

ACKNOWLEDGEMENTS

We thank Trevor Allen for providing advice and Python code to determine Gutenberg-Richter parameters using maximum-likelihood estimation. R code provided by Mignan and Woessner (2012) was adapted to generate the frequency-magnitude distribution plots. Taimi Mulder provided advice on combining catalogs, and Allison Bent provided a useful review. The NRCan Office of Energy Research and Development provided funds for this research. This is an output of the Public Safety Geoscience Program.

REFERENCES

Aki, K. (1965). Maximum Likelihood estimation of b in the formula logN=a-bM and its Confidence Limits. *Bull. Earthquake Res Inst., Tokyo Univ.*, 43, 237-239.

Allen, T. I., J. Adams, S. Halchuk, and G. C. Rogers (in prep, 2016). Documentation for the northern Arctic areal sources and western fault sources for the 5th Generation Seismic Hazard Model of Canada, *Geological Survey of Canada Open File XXXX*, Sidney, Canada.

Argus, D.F., and Peltier, W.R., 2010. Constraining models of postglacial rebound using space geodesy: a detailed assessment of model ICE-5G (VM2) and its relatives, Geophys. J. Int., 181, 697–723 doi: 10.1111/j.1365-246X.2010.04562.x

Basham, P.W., D.A. Forsyth, and R.J. Wetmiller, 1977. The seismicity of northern Canada, Can. J. Earth Sc., 14, 1646-1667.

Bent, A., 2002. The 1933 Ms – 7.3 Baffin Bay earthquake: strike-slip faulting along the northeastern Canadian passive margin, Geophys. J. Int., 150, 724-736.

Chung, W.-Y., 2002. Earthquakes along the Passive Margin of Greenland: Evidence for Postglacial Rebound Control, Pure appl. Geophys., 159, 2567-2584.

GEUS, 2016. Tectonic earthquakes located in Greenland, [Online data file], Available at: http://seis.geus.net/projects/glisn/geus-eqlist.html , accessed Mar. 7, 2016.

GEUS Nordic Format, Available at: http://seis.geus.net/software/seisan/node159.html , accessed March 9, 2016.

Grollimund, B., and M. D. Zoback, 2001. Did deglaciation trigger intraplate seismicity in the New Madrid seismic zone?, Geology, 29, 175-178.

Halchuk, S., Allen, T.I., Rogers, G.C., and Adams, J., 2015. Seismic Hazard Earthquake Epicentre File (SHEEF2010) used in the Fifth Generation Seismic Hazard Maps of Canada; Geological Survey of Canada, Open File 7724. 1 .zip file. doi:10.4095/296908

Ivins, E.R., T.S. James, and V. Klemann, 2003. Glacial isostatic stress shadowing by the Antarctic ice sheet, J. Geophys. Res., 108, 2560, doi:10.1029/2002JB002182.

Johston, A.C., 1987. Suppression of earthquakes by large continental ice sheets, Nature, 330, 467-469.

Malvern, L.E., 1969. Introduction to the Mechanics of a Continuous Medium, Prentice-Hall, Englewood Cliffs, New Jersey, 713 pp.

Mignan, A., J. Woessner (2012), Estimating the magnitude of completeness for earthquake catalogs, Community Online Resource for Statistical Seismicity Analysis, doi:10.5078/corssa-00180805. Available at http://www.corssa.org

Olivieri, M., and G. Spada, 2015. Ice melting and earthquake suppression in Greenland, Polar Science, 9, 94-106.

Peltier, W. R., D. F. Argus, and R. Drummond (2015), Space geodesy constrains ice age terminal deglaciation: The global ICE-6G_C (VM5a) model, J. Geophys. Res. Solid Earth, 119, doi:10.1002/2014JB011176.

Peltier, W., R., and Drummond, R., 2008. Rheological stratification of the lithosphere: A direct inference based upon the geodetically observed pattern of the glacial isostatic adjustment of the North American continent, Geophys. Res. Lett, 35, L16314, doi:10.1029/2008GL034586.

Qamar, A., 1974. Seismicity of the Baffin Bay Region, Bull. Seis. Soc. Am., 64, pp. 87-98.

Simon, K.M., T.S. James, and A.S. Dyke, 2015. A new glacial isostatic adjustment model of the Innuitian Ice Sheet, Arctic Canada, Quat. Sc. Rev., 119, 11-21, http://dx.doi.org/10.1016/j.quascirev.2015.04.007 .

Simon, K.M., James, T.S., Henton, J.A., Dyke, A.S., 2016. A glacial isostatic adjustment model for the central and northern Laurentide ice sheet based on relative sea level and GPS measurements, Geophysical Journal International, 205 (3), ggw098, pp. 1618-1636.

Stein, S. N.H. Sleep, R.J. Geller, S.-C Wang, G.C. Kroger, 1979. Earthquakes along the passive margin of eastern Canada, Geophys. Res. Lett., 6, 537-540.

Wetmiller, R.J., and D.A. Forsyth, 1982. Review of seismicity and other geophysical data near Nares Strait, Meddelelser om Gronnland, Geoscience 8, 261-274.

Wu, P., and H.S. Hasegawa, 1996. Induced stresses and fault potential in eastern Canada due to a disc load: a preliminary analysis, Geophys. J. Int. (1996) 125,415-430.

APPENDIX A. CATALOGUE CHARACTERISTICS

The SHEEF2010 earthquake catalogue (Halchuk et al., 2015) provides the date, preferred magnitude after conversion or estimate, longitude, latitude, name of source agency providing location and magnitude, depth, depth flag, original magnitude, original magnitude type, and the preferred magnitude (to two decimal places).

The GLISN earthquake catalogue provides abundant information on each earthquake using the NORDIC format (GEUS Nordic Format, 2016). It contains 28 columns in an ASCII text format. Attributes matching the SHEEF2010 catalogue were imported from the GLISN catalogue to create a standardized catalogue. Attributes from GLISN that were not carried over to the combined catalogue include information such as the number of stations used to locate the earthquake and the RMS of time residuals.

The combined and complete catalogues developed for this study follow the SHEEF2010 format and are given in a separate data file.